Available online at www.sciencedirect.com

ScienceDirect

Journal of Computational and Applied Mathematics 215 (2008) 512–520

JOURNAL OF COMPUTATIONAL AND APPLIED MATHEMATICS

www.elsevier.com/locate/cam

A numerical solution of a one-dimensional blood flow model—moving grid approach

V. Melicher[a,*], V. Gajdošík[b]

[a] *Department of Mathematical Analysis, Ghent University, Galglaan 2, 9000 Gent, Belgium*
[b] *Laboratoire de physique des rayons X, Ecole Polytechnique Fédérale de Lausanne, 1015 Lausanne, Switzerland*

Received 9 August 2005

Abstract

We consider a one-dimensional blood flow model suitable for larger arteries. It consists of a hyperbolic system of two coupled nonlinear equations. The model has already been successfully used in practice. Its numerical solution is usually achieved by means of an explicit Taylor–Galerkin scheme. We have proposed a different approach. The system can be transformed to characteristic directions emphasizing the physical nature of the problem. We solved this system by using an operator splitting on a moving grid.

Keywords: Blood flow; One-dimensional model; Operator splitting

1. Introduction

The mathematical modelling and the numerical simulations have become important tools for better understanding of the human cardiovascular system in recent years. The range of developed models or models being developed extends from lumped models to complicated three-dimensional fluid-structure models [9,8].

In this article we introduce a one-dimensional model of blood flow in a compliant vessel as described in [4]. The blood flow in the vessel is described by this and generally by all one-dimensional models through averaged quantities. They cannot give us any information about flow pattern. They are also not suitable for describing blood flow in complicated morphological regions as stenosis or bifurcations. However, these situations can also be covered to certain extent [3]. On the other hand computational complexity of one-dimensional models is several orders of magnitude lower than that of multi-dimensional models. Recently, a multi scale approach has attracted wider interest. One-dimensional models may be coupled with lumped parameter models [5] or with two- or three-dimensional fluid models as described for example in [2].

The model presented here is usually solved by means of a second order Taylor–Galerkin scheme, which is a finite element counterpart of the Lax–Wendroff scheme. It is a pure analytic approach, which does not take into account the physical nature of the problem. We have applied an operator splitting approach trying to develop a method suited for this system of equations. We designed a numerical scheme and demonstrate it on examples.

* Corresponding author.
E-mail addresses: valdemar.melicher@ugent.be (V. Melicher), vincent.gajdosik@epfl.ch (V. Gajdošík).

0377-0427/$ - see front matter © 2007 Elsevier B.V. All rights reserved.
doi:10.1016/j.cam.2006.03.065

In Section 2 we review the derivation of the one-dimensional model. Next, we make its complete transformation into characteristic variables.

In Section 3 we review the Taylor–Galerkin scheme for completeness. Further, we introduce the method here developed. Finally, we support it with examples.

2. One-dimensional model

The cylindrical domain Ω_t representing the portion of a vessel is considered to have a static equilibrium in the radial direction. Without loss of generality the axis s is identified with the z coordinate. Γ_1 is the *proximal* (closer to a heart) and Γ_2 the *distal* (further from the heart) boundary (Fig. 1).

By integrating the Navier–Stokes equations on a cross section $S(s,t)$ one gets the following system of two partial differential equations [7]:

$$\left.\begin{aligned} &\frac{\partial A}{\partial t}+\frac{\partial Q}{\partial s}=0\\ &\frac{\partial Q}{\partial t}+\frac{\partial}{\partial s}\left(\alpha\frac{Q^2}{A}\right)+\frac{A}{\rho}\frac{\partial \bar{p}}{\partial s}+K_r\frac{Q}{A}=0 \end{aligned}\right\} \quad s\in(0,l),\ \ t\in(0,T), \tag{2.1}$$

where A, Q and p denote the section area, the average volumetric flux and the mean pressure, respectively,

$$A(t,s)=\int_{S(t,s)}\mathrm{d}\sigma,\quad Q(t,s)=\int_{S(t,s)}u_s\,\mathrm{d}\sigma,\quad \bar{p}(t,s)=\frac{1}{A(t,s)}\int_{S(t,s)}p\,\mathrm{d}\sigma,$$

where u_s denotes the s-component of the velocity. The K_r is a resistance parameter linked to the blood viscosity. The α (Coriolis coefficient) depends on the velocity profile

$$\alpha=A\left(\int_S u_s^2\,\mathrm{d}\sigma\right)\left(\int_S u_s\,\mathrm{d}\sigma\right)^{-2}.$$

It accounts for the fact that the momentum flux computed with the averaged quantities is in general different from the actual momentum flux [5]. For the sake of simplicity it is usually considered constant and equal to one. We follow this usage. Finally, ρ is the density of blood.

The number of unknowns exceeds the number of equations in (2.1). The system can be closed by providing an explicit relation between the pressure p and the vessel area A. We adopt the following relation [4]:

$$\bar{p}=\bar{p}_0+\frac{4\sqrt{\pi}h_0E(s)}{3A_0}(\sqrt{A}-\sqrt{A_0}), \tag{2.2}$$

where $\bar{p}_0$ is the external pressure, A_0 the reference vessel section area, h_0 the wall thickness and $E(s)$ is the Young's modulus of the vessel wall material. We can assume $\bar{p}_0=0$. For the sake of simplicity A_0 is considered constant. Other relations between p and A can be found in [6,11]. We denote

$$\beta(s):=\frac{4\sqrt{\pi}h_0E(s)}{3A_0}.$$

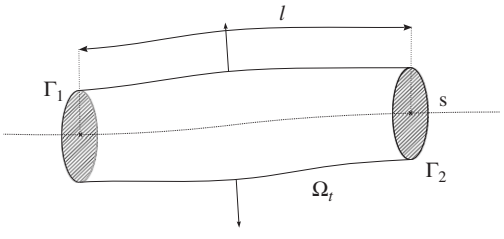

Fig. 1. Domain.

Taking into account (2.2) the system (2.1) can be written in the conservation form

$$\frac{\partial \boldsymbol{U}}{\partial t} + \frac{\partial}{\partial s}\boldsymbol{F}(\boldsymbol{U}) = \boldsymbol{B}(\boldsymbol{U}), \tag{2.3}$$

where

$$\boldsymbol{U} = \begin{bmatrix} A \\ Q \end{bmatrix}, \quad \boldsymbol{F}(\boldsymbol{U}) = \begin{bmatrix} Q \\ \dfrac{Q^2}{A} + \dfrac{\beta}{3\rho}A^{3/2} \end{bmatrix},$$

$$\boldsymbol{B}(\boldsymbol{U}) = \begin{bmatrix} 0 \\ -K_r\dfrac{Q}{A} + \dfrac{A}{\rho}\dfrac{\mathrm{d}\beta}{\mathrm{d}s}\left(\sqrt{A_0} - \dfrac{2}{3}\sqrt{A}\right) \end{bmatrix}. \tag{2.4}$$

Further, it may be written in the quasi-linear form

$$\frac{\partial \boldsymbol{U}}{\partial t} + \boldsymbol{H}\frac{\partial \boldsymbol{U}}{\partial s} = \boldsymbol{B}(\boldsymbol{U}), \tag{2.5}$$

where

$$\boldsymbol{H} = \begin{bmatrix} 0 & 1 \\ c^2 - \left(\dfrac{Q}{A}\right)^2 & 2\dfrac{Q}{A} \end{bmatrix} = \begin{bmatrix} 0 & 1 \\ c^2 - \bar{u}^2 & 2\bar{u}, \end{bmatrix},$$

$$\boldsymbol{B}(\boldsymbol{U}) = \begin{bmatrix} 0 \\ -K_R\dfrac{Q}{A} + \dfrac{A}{\rho}\dfrac{\mathrm{d}\beta}{\mathrm{d}s}(\sqrt{A_0} - \sqrt{A}) \end{bmatrix}. \tag{2.6}$$

Here

$$c^2 = \frac{A}{\rho}\frac{\partial \bar{p}}{\partial A}, \quad \bar{u} = \frac{Q}{A}. \tag{2.7}$$

It may be shown that for all allowable values of $\boldsymbol{U}$, the matrix $\boldsymbol{H}$ possesses two distinct real eigenvalues and a corresponding complete set of two left eigenvectors

$$\lambda_{1,2} = \bar{u} \pm c, \quad \boldsymbol{l}^{1,2} = \frac{1}{A}\begin{bmatrix} -(\bar{u} \mp c) \\ 1 \end{bmatrix}. \tag{2.8}$$

Thus, our system (2.1) is strictly hyperbolic. Moreover, for the values attained by the mechanical parameters and blood velocities in physiologic conditions $c > \bar{u}$. Consequently, the eigenvalues have an opposite sign. Let us denote by $\boldsymbol{L}$ the matrix of left eigenvectors $\boldsymbol{l}^{1,2}$ and $\boldsymbol{\Lambda} = \mathrm{diag}(\lambda_1, \lambda_2)$. Then, we may write

$$\frac{\partial \boldsymbol{U}}{\partial t} + \boldsymbol{L}^{-1}\boldsymbol{\Lambda}\boldsymbol{L}\frac{\partial \boldsymbol{U}}{\partial s} = \boldsymbol{B}(\boldsymbol{U})/\cdot \boldsymbol{L},$$

$$\boldsymbol{L}\frac{\partial \boldsymbol{U}}{\partial t} + \boldsymbol{\Lambda}\boldsymbol{L}\frac{\partial \boldsymbol{U}}{\partial s} = \boldsymbol{L}\boldsymbol{B}(\boldsymbol{U}). \tag{2.9}$$

One can easily find a vector function $\boldsymbol{W}$ such that

$$\boldsymbol{L} = \frac{\partial \boldsymbol{W}}{\partial \boldsymbol{U}} = \begin{bmatrix} \dfrac{\partial W_1}{\partial A} & \dfrac{\partial W_1}{\partial Q} \\ \dfrac{\partial W_2}{\partial A} & \dfrac{\partial W_2}{\partial Q} \end{bmatrix}. \tag{2.10}$$

The functions W_1, W_2 are the *characteristic variables* of the so-called *Riemann invariants*. They can always be found for system of two conservation laws [1]. Here we obtain

$$W_{1,2} = \frac{Q}{A} \pm 2\sqrt{\frac{2}{\rho}} A^{1/4} \beta^{1/2} \tag{2.11}$$

and by inverting

$$A = \left(\frac{\rho}{\beta}\right)^2 \frac{(W_1 - W_2)^4}{4^5}, \quad Q = A\frac{W_1 + W_2}{2}. \tag{2.12}$$

If $\boldsymbol{B} = \boldsymbol{0}$, Eqs. (2.9) decouple

$$\begin{aligned} &\frac{\partial}{\partial t} W_1 + \lambda_1 \frac{\partial W_1}{\partial s} = 0, \\ &\frac{\partial}{\partial t} W_2 + \lambda_2 \frac{\partial W_2}{\partial s} = 0. \end{aligned} \tag{2.13}$$

The authors in [4] used the decoupled system to gain consistent boundary conditions. As $\lambda_1 > 0$, $\lambda_2 < 0$ one can assign only one boundary condition for each end

$$W_1(t) = g_1(t) \ \text{ at } s = 0, \quad W_2(t) = g_2(t) \ \text{ at } s = l. \tag{2.14}$$

The values of W_2 at $s = 0$ and W_1 at $s = l$ can be computed by the extrapolation of the outgoing characteristics. Due to (2.13) one has

$$W_1^{n+1}(l) = W_1^n(-\lambda_1^n(l)\Delta t), \quad W_2^{n+1}(0) = W_2^n(-\lambda_2^n(0)\Delta t), \tag{2.15}$$

where values with index n are known from previous time step. Thus, boundary values of A^{n+1} and Q^{n+1} at $x = 0$ and l can be computed from (2.15) and (2.14) by means of (2.12).

We do not stop at this point and make a full transformation to the characteristic variables. First, let us rewrite the system (2.9) by using (2.10)

$$\frac{\partial \boldsymbol{W}}{\partial \boldsymbol{U}} \frac{\partial \boldsymbol{U}}{\partial t} + \boldsymbol{\Lambda} \frac{\partial \boldsymbol{W}}{\partial \boldsymbol{U}} \frac{\partial \boldsymbol{U}}{\partial s} = \frac{\partial \boldsymbol{W}}{\partial \boldsymbol{U}} \boldsymbol{B}(\boldsymbol{U}). \tag{2.16}$$

By applying the chain rule we gain

$$\frac{\partial \boldsymbol{W}}{\partial s} = \frac{\partial \boldsymbol{W}}{\partial \boldsymbol{U}} \frac{\partial \boldsymbol{U}}{\partial s} + \frac{\partial \boldsymbol{W}}{\partial \beta} \frac{\mathrm{d}\beta}{\mathrm{d}s}.$$

Eventually, by substituting this to (2.16) we obtain

$$\frac{\partial \boldsymbol{W}}{\partial t} + \boldsymbol{\Lambda} \frac{\partial \boldsymbol{W}}{\partial s} = \frac{\partial \boldsymbol{W}}{\partial \boldsymbol{U}} \boldsymbol{B}(\boldsymbol{U}) + \boldsymbol{\Lambda} \frac{\partial \boldsymbol{W}}{\partial \beta} \frac{\mathrm{d}\beta}{\mathrm{d}s}. \tag{2.17}$$

Let us denote

$$\boldsymbol{B}^W := \frac{\partial \boldsymbol{W}}{\partial \boldsymbol{U}} \boldsymbol{B}(\boldsymbol{U}) + \boldsymbol{\Lambda} \frac{\partial \boldsymbol{W}}{\partial \beta} \frac{\mathrm{d}\beta}{\mathrm{d}s}. \tag{2.18}$$

We may write (2.17) componentwise

$$\begin{aligned} &\frac{\partial}{\partial t} W_1 + \lambda_1 \frac{\partial W_1}{\partial s} = \boldsymbol{B}_1^W, \\ &\frac{\partial}{\partial t} W_2 + \lambda_2 \frac{\partial W_2}{\partial s} = \boldsymbol{B}_2^W. \end{aligned} \tag{2.19}$$

The relations (2.12) allow us to express the eigenvalues λ_1, λ_2 and the source term $\boldsymbol{B}^W$ in terms of W_1, W_2. After some rather tedious symbolic computing

$$\lambda_1 = \frac{5W_1 + 3W_2}{8}, \quad \lambda_2 = \frac{5W_2 + 3W_1}{8} \tag{2.20}$$

and

$$\boldsymbol{B}^W = \begin{bmatrix} -512K_R\left(\frac{\beta}{\rho}\right)^2 \frac{(W_1+W_2)}{(W_1-W_2)^4} + \frac{1}{8\rho\beta}(8\sqrt{A_0}\beta + \rho(W_1^2 - W_2^2))\frac{\mathrm{d}\beta}{\mathrm{d}s} \\ -512K_R\left(\frac{\beta}{\rho}\right)^2 \frac{(W_1+W_2)}{(W_1-W_2)^4} + \frac{1}{8\rho\beta}(8\sqrt{A_0}\beta - \rho(W_1^2 - W_2^2))\frac{\mathrm{d}\beta}{\mathrm{d}s} \end{bmatrix}. \tag{2.21}$$

We assumed during the transformation that $W_1 > 0$, $W_2 < 0$, $\rho > 0$, $\beta > 0$.

3. Taylor–Galerkin scheme

As the Taylor-Galerkin method is used as the reference one, we shortly describe it in this section. For the complete derivation we refer the reader again to [4].

The method is a finite element counterpart of the well known Lax–Wendroff (LW) scheme. One obtains the following discretization of (2.3) in time

$$\boldsymbol{U}^{n+1} = \boldsymbol{U}^n - \Delta t \frac{\partial}{\partial s}\left(\boldsymbol{F}^n + \frac{\Delta t}{2}\boldsymbol{F}_{\boldsymbol{U}}^n \boldsymbol{B}^n\right) - \frac{(\Delta t)^2}{2}\left[\boldsymbol{B}_{\boldsymbol{U}}^n \frac{\partial \boldsymbol{F}^n}{\partial s} - \frac{\partial}{\partial s}\left(\boldsymbol{F}_U^n \frac{\partial \boldsymbol{F}^n}{\partial s}\right)\right] + \Delta t\left(\boldsymbol{B}^n + \frac{\Delta t}{2}\boldsymbol{B}_{\boldsymbol{U}}^n \boldsymbol{B}^n\right), \tag{3.1}$$

where

$$\boldsymbol{F}_{\boldsymbol{U}} := \frac{\partial \boldsymbol{F}}{\partial \boldsymbol{U}}, \quad \boldsymbol{B}_{\boldsymbol{U}} := \frac{\partial \boldsymbol{B}}{\partial \boldsymbol{U}}.$$

Let us put $\boldsymbol{F}_{LW} := \boldsymbol{F} + (\Delta t/2)\boldsymbol{F}_{\boldsymbol{U}}\boldsymbol{B}$ and $\boldsymbol{B}_{LW} := \boldsymbol{B} + (\Delta t/2)\boldsymbol{B}_{\boldsymbol{U}}\boldsymbol{B}$. A finite element formulation of (3.1) reads: find $\boldsymbol{U}_h^{n+1} \in \boldsymbol{V}_h$ which satisfies

$$\begin{aligned}(\boldsymbol{U}_h^{n+1}, \boldsymbol{\phi}_h) = (\boldsymbol{U}_h^n, \boldsymbol{\phi}_h) + \Delta t\left(\boldsymbol{F}_{LW}^n, \frac{\partial \boldsymbol{\phi}_h}{\partial s}\right) - \frac{(\Delta t)^2}{2}\left(\boldsymbol{B}_{\boldsymbol{U}}^n \frac{\partial \boldsymbol{F}^n}{\partial s}, \boldsymbol{\phi}_h\right) \\ - \frac{(\Delta t)^2}{2}\left(\boldsymbol{F}_{\boldsymbol{U}}^n \frac{\partial \boldsymbol{F}^n}{\partial s}, \frac{\partial \boldsymbol{\phi}_h}{\partial s}\right) + \Delta t(\boldsymbol{B}_{LW}^n, \boldsymbol{\phi}_h) \quad \forall \boldsymbol{\phi}_h \in \boldsymbol{V}_h^0,\end{aligned} \tag{3.2}$$

where $(.\,,.)$ indicates the inner product in $\mathbf{L}^2((0,l))$, $\boldsymbol{V}_h$ is a suitable finite element space and $\boldsymbol{V}_h^0$ is the set of functions of $\boldsymbol{V}_h$ which are zero at $z = 0$ and l. Von Neumann linear stability analysis for the proposed finite element scheme on a grid with uniform spacing h, gives a stability condition

$$\frac{\Delta t \sup_{0<s<l}(\max_{i=1,2}|\lambda_i|)}{h} < \frac{1}{\sqrt{3}}. \tag{3.3}$$

The method has two shortcomings. The first one is that the LW is a well-known dispersive scheme. The other one is obvious, when the elastic properties of the vessel wall change abruptly, such as in the case of a stent. Consequently β' attains big values. As explained in [3], the use of regularization of β, as done in [4], requires the use of a fine mesh around big jumps of β. This causes a loss of efficiency of LW scheme due to stability condition (3.3).

In [3] the problem of very steep solutions is successfully tackled via the domain decomposition method. But one problem still remains. The LW scheme produces spurious oscillations. It is evident particularly in the case, when the elastic properties of the vessel wall change rapidly, the time step has to be small and number of iterations is substantial. Nevertheless, the oscillations appear always, at least at the front area. One possible solution is to use a flux-limiter method [12], where the LW flux is replaced by a hybrid flux, which behaves as a low order flux near discontinuities and as a high order flux in smooth regions. However, we tried a completely different approach.

4. An operator splitting approach

We have transformed the system (2.1) to the characteristic variables

$$\frac{\partial}{\partial t}W_1 + \frac{5W_1 + 3W_2}{8}\frac{\partial W_1}{\partial s} = \boldsymbol{B}_1^W,$$
$$\frac{\partial}{\partial t}W_2 + \frac{5W_2 + 3W_1}{8}\frac{\partial W_2}{\partial s} = \boldsymbol{B}_2^W, \tag{4.1}$$

with the r.h.s. (2.21). Though the system (4.1) is not in a conservation law form, it is in many aspects rather simpler than (2.1). From the physical point of view the system describes a flow with a source term. The flow speed depends only on the values of W_1 and W_2, moreover linearly. The source term is more complicated. The first term

$$-512K_R\left(\frac{\beta}{\rho}\right)^2\frac{(W_1 + W_2)}{(W_1 - W_2)^4}$$

in $\boldsymbol{B}_{1,2}^W$ is usually in physiological conditions of a small order. But the second term, particularly its part

$$\frac{\sqrt{A_0}}{\rho}\frac{\mathrm{d}\beta}{\mathrm{d}s},$$

causes numerical instability in the situations when the elastic properties of the wall properties change abruptly, such as in the case of a stent.

Let us divide the time interval $(0, T)$ into n subintervals (t_{i-1}, t_i), where $t_i = i\tau$, $i = 1, \cdots, n$ and $\tau = T/n$ is the time step. We employ an operator splitting idea. First, we solve the problem at one time interval for convection and subsequently the resulting system of ODEs. The method of characteristics in this setting reads

$$\frac{W_1^{n+1,(k)} - W_1^n \circ \phi_1^{n,(k-1)}}{\tau} = B_1(W_1^{n+1,(k-1)}, W_2^{n+1,(k-1)}),$$
$$\frac{W_2^{n+1,(k)} - W_2^n \circ \phi_2^{n,(k-1)}}{\tau} = B_2(W_1^{n+1,(k-1)}, W_2^{n+1,(k-1)}), \tag{4.2}$$

where $W_i^{n,(k)}$ stands for approximation of the solution W_i at time $t = n\tau$ gained by kth iteration and $\phi_i^{n,(k)}$ stands for approximation of the characteristics

$$\phi_i^{n,(k-1)} = x - \tau\lambda_i(W_1^{n+1,(k-1)}, W_2^{n+1,(k-1)}), \tag{4.3}$$

where $W_i^{n+1,(0)} = W_i^n$. In practical realization of the last relation we used instead of $W_i^{n+1,(k-1)}$ the averaged value

$$\frac{W_i^{n+1,(k-1)} + W_i^n}{2}.$$

The second equation of (4.2) may be modified

$$\frac{W_2^{n+1,(k)} - W_2^n \circ \phi_2^{n,(k-1)}}{\tau} = B_2(W_1^{n+1,(k)}, W_2^{n+1,(k-1)}), \tag{4.4}$$

as the $W_1^{n+1,(k)}$ is already known. Eq. (4.2) is in fact the *backward Euler* scheme.

As said before, the physical nature of the problem is a flow with a source term. If it is solved on a fixed grid, the justice to the physical nature is not done. Thus, we solved (4.2) on a moving grid. Let us call the resulting scheme the point tracking (PT), as we first move the grid and subsequently solve the system of ODEs.

5. Numerical results

From (2.2) and (2.12) we get ($\bar{p} = 0$)

$$W_1 = W_2 + 4\sqrt{\frac{2}{\rho}}\left(\sqrt{p + \beta\sqrt{A_0}}\right). \tag{5.1}$$

So we can enter the proximal boundary condition in terms of a pressure impulse

$$g_1(t) = W_2(0, t) + 4\sqrt{\frac{2}{\rho}}\left(\sqrt{\xi(t) + \beta(0)\sqrt{A_0}}\right), \tag{5.2}$$

or

$$g_1(t) = W_2(0, 0) + 4\sqrt{\frac{2}{\rho}}\left(\sqrt{\xi(t) + \beta(0)\sqrt{A_0}}\right), \tag{5.3}$$

when we suppose that the proximal boundary is non-reflexive.

As a pressure impulse we used a sine wave depicted in Fig. 2.

In Fig. 3 we encounter spurious oscillations produced by the LW scheme. We took the time step $\tau = 10^{-6}$ s to emphasize this behaviour. As mentioned earlier, this in fact means we cannot use the method for very steep solutions or longer intervals.

The comparison of the proposed method (PT) and the LW scheme can be found in Fig. 4. Even if the time interval τ is taken almost optimal in order to fulfill (3.3), we can see small oscillations in the front area produced by the LW.

Next, we simulate the change of the wall properties. We consider the example used in [4]. The length of the vessel portion is 15 cm and the β depicted in Fig. 5 is used. This describes a situation, when for example a stent is applied. We would like to refer the reader to an interesting solution of the problem using discontinuous Galerkin [10]. The region where the vessel wall is stiffer is $j_1 \leqslant x \leqslant j_2$, where $j_1 = 5$ cm and $j_2 = 10$ cm. The jumps at these points are regularized. The third order polynomials are used. The constant K determines how stiff the walls are. Using the data from [4] $\beta_0 = 451\,352$. We take $K = 1.2$ such that jump of β is 90 270. The width of the jump area $\delta = 1$ and the time step is $\tau = 10^{-4}$. Fig. 6 shows the solution at different time steps. The area where the vessel wall is stiffer is easily identifiable. Small irregularities can be seen at the jump points, particularly in the depiction of the flux Q. Some adaptation of the moving grid could be used to improve the accuracy at the regions where the solution is very steep. It can be done by adapting the time step for each grid point depending on a certain measure of steepness. Thus, in contrast to the LW the refinement can be decided locally, which improves the efficiency.

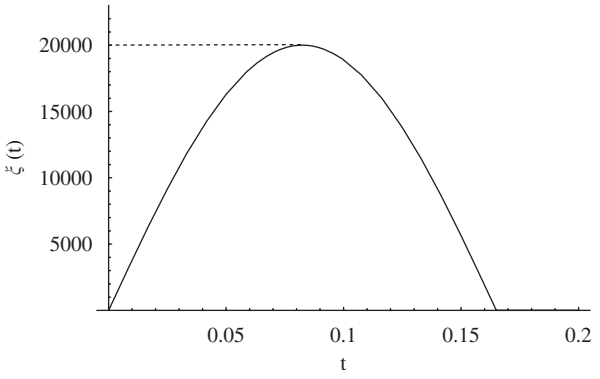

Fig. 2. Pressure $\xi(t)$.

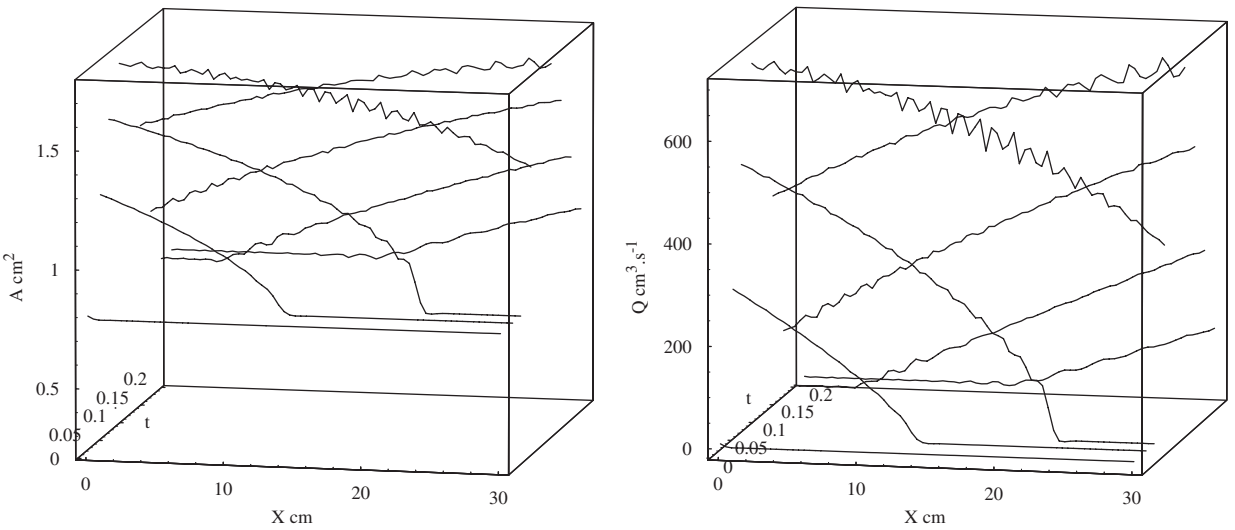

Fig. 3. *Lax–Wendroff*, $l = 30\,\text{cm}$, $n = 60$, $h = 0.5\,\text{cm}$, $\tau = 10^{-6}\,\text{s}$, $\beta = \text{const}$.

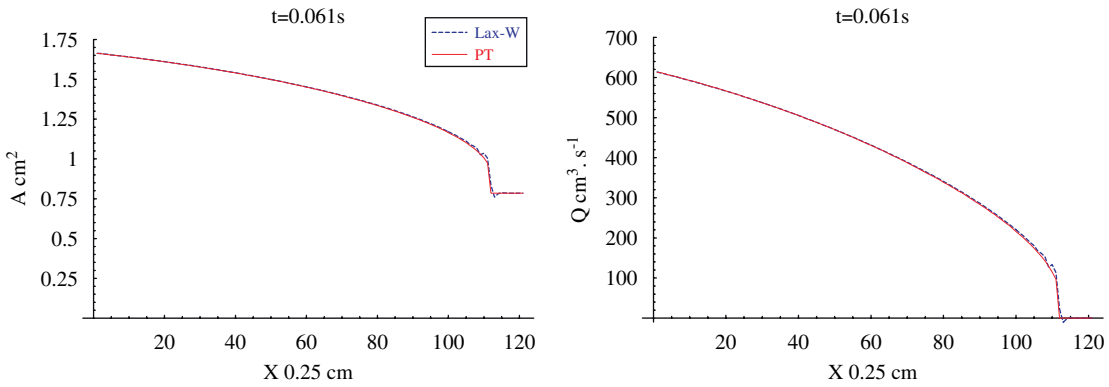

Fig. 4. LW versus PT, $l = 30\,\text{cm}$, $n = 120$, $h = 0.25\,\text{cm}$, $\tau = 10^{-4}\,\text{s}$, $\beta = \text{const}$.

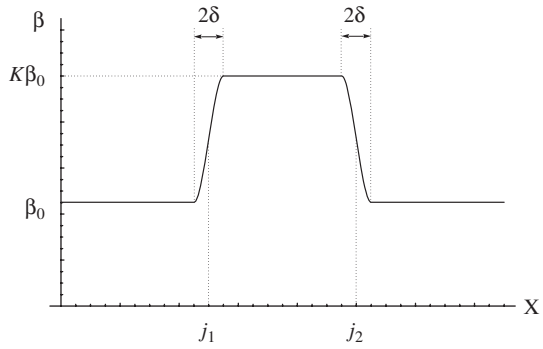

Fig. 5. Beta.

Remark 1. The use of moving grid causes many algorithmic difficulties. Particularly, it is costly to ask for value of the solution $W_i(x)$, $i \in 1, 2$ at the certain point x. One should always avoid it.

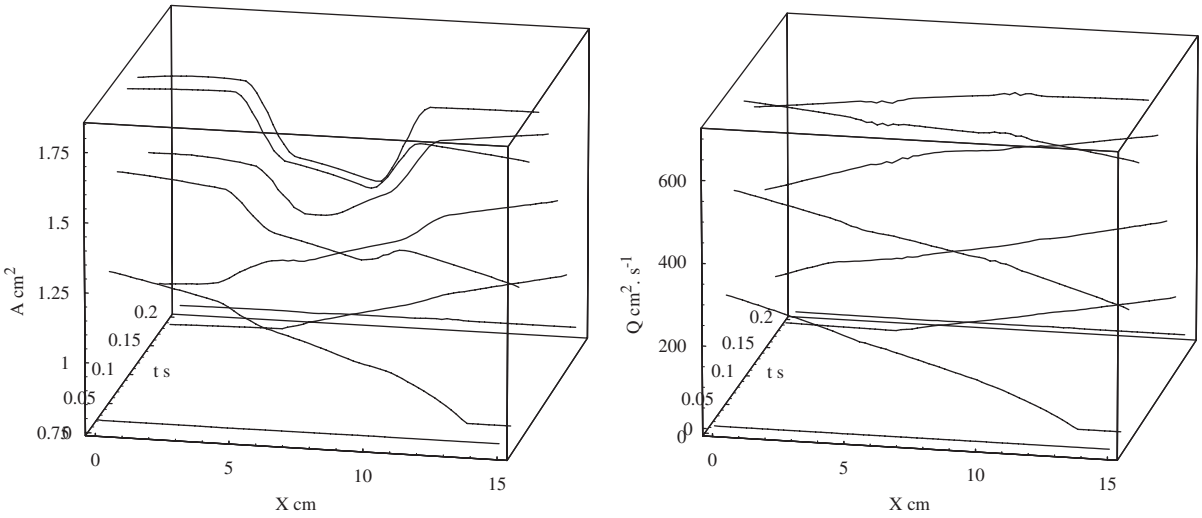

Fig. 6. PT, $l = 15\,\text{cm}$, $\tau = 10^{-4}\,\text{s}$.

6. Conclusion

We transformed a one-dimensional blood flow model to the characteristic variables and applied the operator splitting idea to the resulting system. To satisfy the flow nature of the problem, the spatial discretization by a moving grid was applied. The approach resulted in an oscillation free method, comparable to the often used Lax–Wendroff scheme. The effectiveness could be improved by time step adaptation. However, an effective implementation requires certain state-of-art programming techniques.

References

[1] L.C. Evans, Partial Differential Equations, American Mathematical Society, Providence, RI, 1998.
[2] L. Formaggia, J.-F. Gerbeau, F. Nobile, A. Quarteroni, On the coupling of 3D and 1D Navier–Stokes equations for flow problems in compliant vessels, Comput. Methods Appl. Mech. Eng. 191 (6–7) (2001) 561–582.
[3] L. Formaggia, D. Lamponi, A. Quarteroni, One dimensional models for blood flow in arteries, J. Eng. Math. 47 (3–4) (2003) 251–276.
[4] L. Formaggia, F. Nobile, A. Quarteroni. A one dimensional model for blood flow: application to vascular prosthesis, in: I. Babuska, T. Miyoshi, P.G. Ciarlet (Eds.), Mathematical Modeling and Numerical Simulation in Continuum Mechanics, Lecture Notes in Computational Science and Engineering, vol. 19, Springer, Berlin, 2002, pp. 137–153.
[5] L. Formaggia, F. Nobile, A. Quarteroni, A. Veneziani, Multiscale modelling of the circulatory system a preliminary analysis, Comput. Visualisation Sci. 2 (1999) 75–83.
[6] G. Langewounters, K. Wesseling, W. Geodhard, The elastic properties of 45 human thoracic and 20 abdominal aortas in vitro and the parameters of a new model, J. Biomech. 17 (1984) 425–435.
[7] A. Quarteroni, L. Formaggia, Mathematical modelling and numerical simulation of the cardiovascular system, in: Modelling of Living Systems, Handbook of Numerical Analysis, vol. 19, Elsevier Science, Amsterdam, 2002.
[8] A. Quarteroni, M. Tuveri, A. Veneziani, Computational vascular fluid dynamics problems, models and methods, Comput. Visualisation Sci. 2 (2000) 163–197.
[9] V. Rideout, D. Dick, Difference-differential equations for fluid flow in distensible tubes, IEEE Trans. Biomed. Eng. BME 14 (1967) 171–177.
[10] S.J. Sherwin, L. Formaggia, J. Peiró, V. Franke, Computational modelling of 1D blood flow with variable mechanical properties and its application to the simulation of wave propagation in the human arterial system, Int. J. Numer. Meth. Fluids 43 (6–7) (2003) 673–700.
[11] A. Tozeren, Elastic properties of arteries and their influence on the cardiovascular system, ASME J. Biomech. Eng. 106 (1984) 182–185.
[12] R. Veque, Numerical Methods for Conservation Laws, Springer, New York, 1992.